Conformations and Barriers of Haloethyl Radicals (CH_2XCH_2, X = F, Cl, Br, I): Ab Initio Studies

Hyotcherl Ihee,[†] Ahmed H. Zewail,[†] and William A. Goddard III*,[‡]

Arthur Amos Noyes Laboratory of Chemical Physics (127-72), and Materials and Process Simulation Center, Beckman Institute (139-74), Division of Chemistry and Chemical Engineering, California Institute of Technology, Pasadena, California 91125

Received: March 12, 1999; In Final Form: June 8, 1999

Radicals such as $CH_2XCH_2^•$, where X is a halogen, play an important role in the stereochemical control observed in many chemical reactions. To elucidate the origin of the stereoselectivity, we calculated the structures and potential energy surfaces of the haloethyl radicals ($CH_2XCH_2^•$, X = F, Cl, Br, I) using ab initio quantum mechanics [HF, local MP2, DFT (both B3PW91 and B3LYP)]. We find that the $CH_2BrCH_2^•$ and $CH_2ICH_2^•$ radicals strongly favor the symmetrically bridged structures while the $CH_2ClCH_2^•$ radical leads to similar energy for symmetric bridging and classical structures. (In contrast, X = H and F leads to dramatically different structures). This confirms the Skell hypothesis of symmetric bridging to explain the stereochemical control of the $CH_2BrCH_2^•$ and $CH_2ICH_2^•$ radicals, indicating that such bridged structures play an important role in the dissociation processes involving $CH_2XCH_2^•$ with X = Cl, Br, and I. The trends in the rotational barriers and structural parameters are consistent with hyperconjugation between the singly occupied carbon 2p orbital and the σ^*(C-X) MO. We find that the rotational barrier, bridged structure, and dissociation of the radicals are described much more accurately using DFT (with GGA) than with HF or LMP2.

1.0. Introduction

The class of halo radicals such as $CH_2XCH_2^•$ is important in a number of chemical processes[1−4] and determines the stereoselectivity of the reaction products from halogenation[1,2,5−9] of alkenes and alkanes. Their role in stereoselective control is determined by whether the radical is classical (Figure 1c) or bridged and if bridged whether the structure is symmetric (Figure 1a) or asymmetric (Figure 1b). The possible minima and transition structures for rotation around the C−C bond are schematically represented in Figure 2. Anti (I) and gauche (III) rotamers are candidates for local energy minima on the rotational energy surface because Pauli repulsion between bonding pairs would be minimized at these two conformations. The other two structures (II and IV) possessing eclipsed bonds are also possible transition states on the rotational energy surface.

If the structure of the radical is bridged, we expect retention of the stereochemistry. However, if the radical prefers a classical asymmetric conformation, additional conditions must be fulfilled to exert stereochemical control. Namely, a strong preference for high population of the anti conformer and nonplanarity of the radical center are required. Experimental[10−20] and theoretical[21−43] studies have led to a good understanding of the structure and energetics for the cases of X = H, F, and Cl; however, little is known about X = Br and I. The motivation for our studies was to elucidate the X = Br and I systems. But we also studied X = H, F, Cl in cases to compare to previous experiments and theory.

In this paper we use four techniques of first principles quantum mechanics (QM) methods to examine the potential surface for $CH_2XCH_2^•$ with X = H, F, Cl, Br, and I. These QM methods are HF, local MP2 (LMP2), and two kinds of DFT (B3LYP and B3PW91). We find that X = Br and I are significantly different from the cases of X = H, F, and Cl.

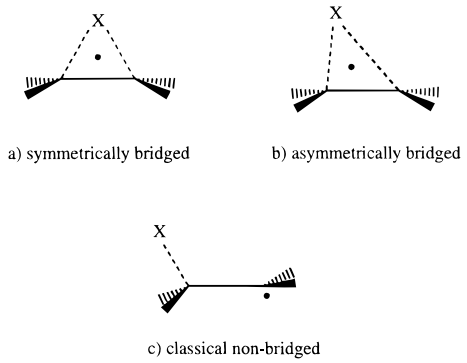

Figure 1. Hypothesized structures for β-substituted alkyl radical. (a) Symmetrically bridged, (b) asymmetrically bridged, and (c) classical non-bridged.

Section 2 reviews the current level of understanding for these systems. Section 3 explains the QM methods being used, and section 4 presents the results.

2.0. Previous Studies

2.1. Experiments. It is well established that the carbonium ion $C_2H_4X^+$ (where X = H, F, Cl, Br, I) has a bridged structure with one X^+ shared equally between the two carbons.[44−46] However, there is no general agreement on whether the radical $C_2H_4X^•$ is bridged.[47] On the basis of the stereochemical control observed in the free radical addition of HBr to 1-bromocyclohexene and 1-methylcyclohexene, Goering et al.[5] introduced the concept of a bridged radical to explain the results. Also, Thaler[6]

* To whom correspondence should be addressed (E-mail: wag@wag.caltech.edu).
[†] Arthur Amos Noyes Laboratory of Chemical Physics.
[‡] Materials and Process Simulation Center.

10.1021/jp990867n CCC: $18.00
Published on Web 07/28/1999

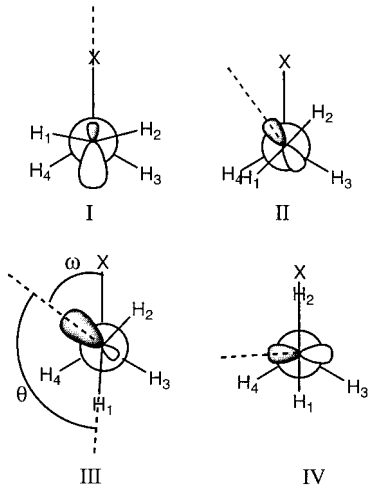

Figure 2. A schematic view of the possible rotational minima and the transition structures of the CH_2XCH_2 (X = F, Cl, Br, and I).

reported the unexpected preponderance of *trans*-1,2-dibromide in the product mixture from the radical bromination of several alkyl bromides and suggested that the intermediate bromoalkyl radical may exist as a three-membered ring species. To understand this stereoselectivity, many researchers have studied the β-substituted alkyl radicals both experimentally[10−20] and theoretically.[21−43]

Three possible structures (Figure 1) could play a role in the stereochemical retention observed in many reactions containing β-haloalkyl radicals:[47]

(a) symmetrically bridged radical, (b) asymmetrically bridged radical, and (c) classical radical (asymmetric and nonbridged).

The early proposal by Goering et al. did not distinguish between symmetrically or asymmetrically bridged species. Later, Skell and co-workers[7,48] advocated a *symmetrically* bridged structure for β-substituted alkyl radicals containing third- and higher row elements to explain the stereochemical control observed in many reactions. However, on the basis of the hyperfine coupling constants from the ESR spectrum, Bowles et al.[13] suggested that the β-chloroethyl radical prefers the anti conformation in which the Cl atom is in the same plane as the singly occupied carbon 2p orbital. Also, Kochi and co-workers[49] disputed Skell's hypothesis based on the inequivalence of α- and β-splittings of ESR spectrum in $R_nMCH_2CH_2^\bullet$ radicals containing third- and higher row elements. Instead, they suggested asymmetrically bridged structures. Semiempirical INDO calculations[43] on ethyl and β-chloroethyl radicals supported this asymmetric bridging hypothesis. However, β-bromo and β-iodo radicals have not been identified by ESR,[10] hence, the argument of Kochi and co-workers cannot be applied generally. In response, Skell and co-workers[47] suggested that stereochemical control could be explained also with a *dynamic* asymmetric bridging (shuttle motion) where the substituent oscillates rapidly between the two carbon atoms. Alternatively, Lloyd and Wood[50] pointed out that the stereoselectivity can be explained in terms of a high rotational barrier around the C−C bond in conjunction with a nonplanar radical center for β-chloro, β-bromo, and β-iodo alkyl radicals (based on the ESR study of β-halo-*tert*-butyl radicals and INDO calculations). Most investigations using ESR techniques have been limited to β-substituted radicals containing H, F, Cl, S, Si, and Sn as a substituent. For the $CH_2FCH_2^\bullet$ radical, Chen et al.[12] observed unusual selective line broadening in the ESR spectra and strong temperature dependence of the β-proton and β-fluorine coupling constants. They suggested that a rapid interconversion takes place between two or more different equilibrium conformations which differ in energy by <0.3 kcal/mol and which are separated by a barrier <1.5 kcal/mol. Edge and Kochi[10] could not observe the β-bromoalkyl (both the β-bromoethyl and the β-bromopropionyl) radical in solution even at $-120°$ by ESR. As they pointed out, their inability to observe the ESR spectra of the β-bromoalkyl radical *in solution* does not indicate that such is not possible. For example, the ESR spectra of β-bromo and β-iodoalkyl radicals were obtained in frozen solution at 77 K by ^{60}Co γ-radiolysis.[51]

2.2. Theoretical Studies. Since the experimental results hardly distinguish the possibilities, many theoretical calculations have been performed to determine the most stable structures. Most theoretical studies have been devoted to the β-fluoroethyl radical ($CH_2FCH_2^\bullet$)[21−36] and to the β-chloroethyl radical ($CH_2ClCH_2^\bullet$)[31−43] with very little attention to the β-bromoethyl radical ($CH_2BrCH_2^\bullet$)[35] and β-iodoethyl radical ($CH_2ICH_2^\bullet$).

2.2.1. $CH_2FCH_2^\bullet$. Early ab initio calculations[27−29,36] generally considered only two structures; the eclipsed structure (IV in Figure 2), where the carbon 2p orbital is perpendicular to the FCC plane, and the anti structure (I in Figure 2), where the 2p orbital is coplanar with FCC plane. Pople and co-workers[29] studied the rotational barriers in substituted ethyl radicals using ab initio unrestricted HF (UHF) calculations with a minimal basis set (STO-3G). They pointed out that the barriers of the radicals are smaller than those of corresponding cations. For the $CH_2FCH_2^\bullet$ radical, their calculation showed no energy difference between the eclipsed form and the anti conformation. They rationalized the general decrease of rotational barrier in the radicals by suggesting that the hyperconjugative interaction between the 2p($CH_2^\bullet$) orbital and the $\pi_x(CH_2F)$ or $\pi_y(CH_2F)$ orbital at the β-carbon is reduced in the radicals because the 2p orbital is no longer vacant. Pross and Radom[28] reported UHF calculations (UHF/4-31G or UHF/5-31G) of β-substituted ethyl radicals where the substituents are second-row elements. They observed that the eclipsed form shows only slight conformational preferences (0.6 kcal/mol) to the anti conformation of $CH_2FCH_2^\bullet$ and rationalized such behavior in terms of opposing changes in positive and negative hyperconjugation between the CH_2F group and the $CH_2^\bullet$ center. In contrast, Kato and Morokuma[27] reported that the eclipsed form is the saddle point for the internal rotation around the C−C bond while the anti structure is the minimum (at the UHF/4-31G level of calculation).

Fossey and Nedelec[26] used the UHF method with the STO-3G basis set to study 1,2-migrations observed in many free radical reactions. They considered only the anti conformation and the symmetrically bridged form. They reported that they could not find an energy minimum for the bridged structure of the $CH_2FCH_2^\bullet$ radical. Schlegel[25] studied the $F + C_2H_4$ reaction by fully optimizing the equilibrium geometries and transition structures using UHF/3-21G, HF/6-31G*, and MP2/3-21G methods. In contrast with previous ab initio calculations, they reported that the CH_2FCH_2 radical adopts a gauche conformation (III in Figure 2). They also reported that the anti structure is at the saddle point with one imaginary vibrational frequency at the UHF/3-21G level. On the basis of UHF and MP2 calculations, Clark and co-workers reported that protonation[34] and addition of a metal cation[52] enhance the stability of the symmetrically bridged structures. Bernardi and co-workers[24,32] used perturbational MO approaches to rationalize the conformational preference in β-substituted ethyl radical in the framework of the UHF calculations. They suggested that the hyperconjugation between the singly occupied carbon 2p orbital and the σ^*(C-X) MO plays the major role in determining the

preferred conformation. Engels and Peyerimhoff[22] reported that the bridged form of $CH_2FCH_2^\bullet$ is stable with respect to the dissociation but too high to allow any shuttle motion in their large scale multireferenced configuration interaction (MRD-CI) calculation. They found only one minimum (gauche form) along the rotation around the C−C bond. In contrast, Tschuikow-Roux and co-workers[53] reported there are two minima and two saddle points along the rotational surface at the UHF and MP2//UHF levels of theory.

2.2.2. $CH_2ClCH_2^\bullet$. On the basis of INDO calculations, Biddles and Hudson[43] claimed that the β-chloroethyl radical has a Cl−C−C bond angle of 92°, supporting the asymmetric bridged structure proposed by Kochi and co-workers.[49] Except for this early INDO calculation, there seems to have been no ab initio calculations supporting an asymmetrically bridged structure for the $CH_2ClCH_2^\bullet$ radical. Hopkinson et al.[42] performed UHF/4-31G* calculations on CH_2ClCH_2 with minimal and split-valence shell basis sets. They reported a rotational barrier of 2 kcal/mol and concluded that there is no evidence of bridging for the Cl atom. Molino et al.[36] studied the conformational preferences and structural trends for a series of fluorine- and chlorine-substituted methyl and ethyl radicals using MNDO type calculations with UHF and half-electron formalisms. Their calculations suggested that the CH_2FCH_2 radical prefers the eclipsed conformation and the CH_2ClCH_2 radical prefers the anti conformation. Fossey and Nedelec[26] reported that the bridged CH_2ClCH_2 radical is 53 kcal/mol higher than the anti structure. Schlegel et al.[41] studied the $Cl + C_2H_4$ reaction using UHF/3-21G*, HF/6-31G*, and MP2/3-21G methods and reported that the CH_2ClCH_2 radical adopts an anti conformation with a rotational energy barrier of 4 kcal/mol. Hoz et al.[40] studied the 1,2-rearrangement in β-substituted ethyl radicals using active space multiconfiguration self-consistent field calculations. They reported that the symmetric bridged structure is above the $Cl + C_2H_4$ dissociation energy limit, suggesting that symmetric bridging in CH_2ClCH_2 is not likely. In contrast, Engels et al.[38] performed large-scale MRD-CI calculations and reported that the symmetrically bridged form is stable to the dissociation and only 6.2 kcal/mol higher than the anti conformation. Recently, Tschuikow-Roux and co-workers studied the rotation/inversion barriers of CH_2ClCH_2.[37] They reported that the rotational barrier for CH_2ClCH_2 is only 1.5 kcal/mol at the MP2/6-311G*//HF/6-31G* level with the anti conformation preferred. They did not study the bridged structure for the radicals.

2.2.3. $CH_2BrCH_2^\bullet$. On the basis of ab initio large scale MRD-CI studies of the β-haloethyl radicals for X = F, Cl, and Br, Engels and Peyerimhoff[35] reported that the absolute minimum in the potential energy surface is an asymmetric radical for all three cases. The structures of the asymmetric radicals in their calculations did not show evidence for asymmetric bridging. On the basis of the energy difference between the absolute minimum and the symmetric conformation, they suggested that the shuttle motion is highly probable in CH_2BrCH_2 but less favorable for CH_2FCH_2 and CH_2ClCH_2. It should be noted that the shuttle motion in the Engels and Peyerimhoff discussion is different from Skell's dynamic asymmetric bridging in that the latter refers to the rapid oscillation between two asymmetrically bridged radicals while the former involves a symmetrically bridged structure between two asymmetric nonbridged radicals (classical radicals).

In the most recent study on the β-substituted ethyl radicals, Guerra[31] concluded that the observed stereochemical control could be accounted for by (i) a high population of the anti conformer in radicals bearing third-row substituents in conjunction with the nonplanarity of the radical site and/or (ii) steric hindrance of the β-substituent due to bridging.

To distinguish between these two possibilities for explaining the stereoselective control, it is important to study simultaneously the rotational barrier and the stability of the bridged structure. The CH_2BrCH_2 and CH_2ICH_2 radicals have rarely been studied by ab initio methods. We know of just one ab initio study[35] on the CH_2BrCH_2 radical and could not find any theoretical study on the CH_2ICH_2 radical. Moreover, simultaneous studies on both the bridged structure and the rotational barrier have been sparse and no systematic study encompassing all the β-substituted haloethyl radicals has been reported. This contribution is meant to remedy this situation.

3.0. Calculations

All calculations were performed using the Jaguar 3.0 program,[54] which utilizes pseudospectral algorithms. The H, C, and F atoms were described using the 6-31G** basis set. The I, Br, and Cl atoms were described using the LAV3P relativistic effective core potential (RECP)[55] and basis set. The LAV3P basis set consists of 3s3p1d valence primitive Gaussian functions contracted to 3s2p1d. The RECP was based on atomic calculations including relativistic effects.

For each system, the geometry was optimized at three levels of theory restricted to be proper spin states: (1) Hartree−Fock (HF), (2) second-order local Møller−Plesset[56] perturbation theory (LMP2) to account for electron correlation, and (3) density functional theory (DFT).

In addition, we carried out LMP2 calculations[57,58] at the optimized HF geometry, denoted LMP2//HF. We did not include spin−orbital coupling. This has negligible effect for the molecular radials since the states are orbitally nondegenerate. For the dissociated halo radials, the calculated bond energies should be decreased by $\sim(1/3)E(^2P_{1/2} - {}^2P_{3/2})$. This is significant only for iodine, where the adiadatic bond energy would be ~8 kcal/mol lower.

Two flavors of DFT method were used, B3PW91 and B3LYP. Both include gradient corrections, exact HF exchange, making them much more accurate than the simple local density approximation (LDA). B3LYP employs a combination of exchange terms: exact HF, the Becke 1988 nonlocal gradient correction,[59] and the original Slater local exchange functional.[60] In addition, it uses the Vosko−Wilk−Nusair (VWN) local functional[61] and the Lee−Yang−Parr local and nonlocal electron correlation functional.[62] B3PW91 uses the same exchange functional as B3LYP but uses the Perdew−Wang 1991 local correlation functional and the GGA-II nonlocal correlation functional.[63]

For the minima and transition states, we calculated harmonic vibrational frequencies at the HF, B3PW91, and B3LYP levels of theory. This was used to obtain the zero point energy. All minima were found to have all real frequencies and all transition states were found to have just one imaginary frequency except for the case of the $CH_2FCH_2^\bullet$ radical. The relative energies and dissociation energies were corrected for the zero point energy using a scaling factor of 0.92 for HF and 0.98 for DFT methods. For the LMP2//HF and LMP2 calculations, we used the HF zero point corrections. All (unscaled) zero point energies and total energies are provided in Table 1.

4.0. Results for β-substituted Haloethyl Radicals; CH_2XCH_2 (X = F, Cl, Br, I)

4.1. Asymmetric Structures and the Rotational Barriers. To find the global minima and correlate the structural changes

TABLE 1: Total Energy (Hartree) of CH_2XCH_2 Radicals Calculated at Various Levels of Theory[a]

method	C_2H_4	I	Br	Cl	F	H
HF	−78.03887 (34.19)	−11.15723	−12.91863	−14.68120	−99.36175	−0.49823
LMP2//HF	−78.31376	−11.17128	−12.93869	−14.70823	−99.48943	−0.49823
LMP2	−78.31430 (32.89)	−11.17128	−12.93869	−14.70823	−99.48943	−0.49823
B3PW91	−78.56139 (32.10)	−11.38531	−13.15084	−14.91530	−99.67926	−0.50217
B3LYP	−78.59380 (32.07)	−11.36306	−13.13069	−14.89608	−99.71429	−0.50027

method	a−CH_3CH_2 (I)	te-CH_3CH_2 (IV)
HF	−78.60129 (39.75)	−78.60072 (39.07)
LMP2//HF	−78.87128	−78.87102
LMP2	−78.87139	−78.87108
B3PW91	−79.13431 (37.43)	−79.13416 (37.17)
B3LYP	−79.16369 (37.35)	−79.16354 (37.08)

method	a-CH_2FCH_2 (I)	g-CH_2FCH_2 (III)	tex-CH_2FCH_2 (IV)	teh-CH_2FCH_2 (II)
HF	−177.44560 (35.76)	−177.44600 (35.65)	−177.44535 (35.24)	−177.44526 (34.87)
LMP2//HF	−177.87046	−177.87244	−177.87218	−177.87082
LMP2	−177.87101	−177.87324	−177.87293	converge to I
B3PW91	−178.31942 (33.58)	−178.32024 (33.29)	−178.31993 (32.81)	converge to I
B3LYP	−178.38507 (33.49)	−178.38582 (33.19)	−178.38549 (32.70)	converge to I

method	a-CH_2ClCH_2 (I)	b-CH_2ClCH_2	te-CH_2ClCH_2 (IV)
HF	−92.72628 (34.89)	−92.72150 (34.55)	−92.72221 (33.68)
LMP2//HF	−93.02238	−93.02078	−93.01971
LMP2	−93.02272	−93.02137	−93.01986
B3PW91	−93.50166 (32.89)	−93.49428 (32.86)	−93.49547 (31.94)
B3LYP	−93.50936 (32.77)	−93.50664 (32.86)	−93.50220 (31.82)

method	a-CH_2BrCH_2 (I)	b-CH_2BrCH_2	te-CH_2BrCH_2 (IV)
HF	−90.94928 (34.55)	−90.95898 (34.57)	−90.94336 (33.25)
LMP2//HF	−91.23914	−91.25103	−91.23406
LMP2	−91.23956	−91.25164	−91.23488
B3PW91	−91.72445 (32.62)	−91.72603 (32.93)	−91.71438 (31.57)
B3LYP	converge to bridge	−91.73727 (32.82)	−91.71997 (31.46)

method	a-CH_2ICH_2 (I)	b-CH_2ICH_2	te-CH_2ICH_2 (IV)
HF	−89.17801 (34.30)	−89.19758 (34.57)	−89.17114 (32.99)
LMP2//HF	−89.46416	−89.48363	−89.45770
LMP2	−89.46458	−89.48425	−89.45832
B3PW91	converge to bridge	−89.95607 (32.88)	−89.93640 (31.49)
B3LYP	converge to bridge	−89.96520 (32.70)	−89.93985 (31.24)

[a] The unscaled zero point energies (kcal/mol) are also presented in parentheses. The anti conformer has a prefix of a- and the eclipsed form has a prefix of te-. The symmetrically bridged structure has a prefix of b-.

with the relative energies between each conformation, we optimized the geometries at a HF level as a function of the torsion angle ω at 5° steps. Single point calculations with LMP2, B3PW91, and B3LYP methods were then performed at the geometries optimized at the HF level of theory. Figure 3 displays the resulting rotational energy curves. Then, the geometries of the minima and the transition structures were fully optimized also at LMP2, B3PW91, and B3LYP levels of theory. The calculated total energies at minima and transition states are given in Table 1 and the relative energies are provided in Table 2. The optimized structures at various levels of theory are presented in Table 3.

At all levels of calculations, the CH_2ClCH_2, CH_2BrCH_2 and CH_2ICH_2 radicals have only one minimum [the anti conformation (I)] and only one transition state (IV). In contrast, the CH_2FCH_2 radical shows different behavior for the various methods. The HF calculation finds two minima (I and III) and two transition states (II and IV) while the LMP2 and DFT calculations show only one minima (III) and two saddle points (I and IV).

All methods give somewhat similar overall descriptions of the various CH_2XCH_2 cases. Thus, in all cases: (1) X = H slightly favors anti (with $\omega = 0°$); the rotational barrier through the IV* rotamer is less than 0.2 kcal/mol except for HF. (2) X = F rather strongly favors gauche (III) with $\omega = 64-70°$. Here the barrier through the IV* rotamer ($\omega = 90°$) ranges from 0.16 to 0.4 kcal except for HF. While HF finds a minimum at the anti conformation ($\omega = 0°$), the MP2 and DFT calculations do *not* lead to a minima; they find a saddle point instead. (3) X = Cl, Br, I strongly favors the anti ($\omega = 0°$) conformation and the rotational barrier through the IV rotamer increases in the order of Cl, Br, and I.

For the C_2H_5 and CH_2FCH_2 radicals, the internal rotation is almost free. Our HF results on the CH_2FCH_2 radical generally agree with the estimates based on ESR data[12] and are close to the results from recent ab initio calculations at the UHF and MP2//HF levels of theory by Tschuikow−Roux and coworkers.[21] In contrast, the LMP2 and DFT methods give only one stable conformation (gauche) rather than two minima (anti and gauche) for CH_2FCH_2. Instead, the anti structure is located at the saddle point at the LMP2 and DFT methods. There is no general agreement on the nature of the anti rotamer. Some[25,32] previous ab initio calculations suggest a saddle point for the anti structure ($\omega = 0°$) while others[21,31] find a minimum there. For the C_2H_5 and CH_2FCH_2 radicals only, the energy difference between rotamers is comparable to the difference of the zero point energies. Indeed, some of the rotational barriers become negative after the correction for the zero point energies. This

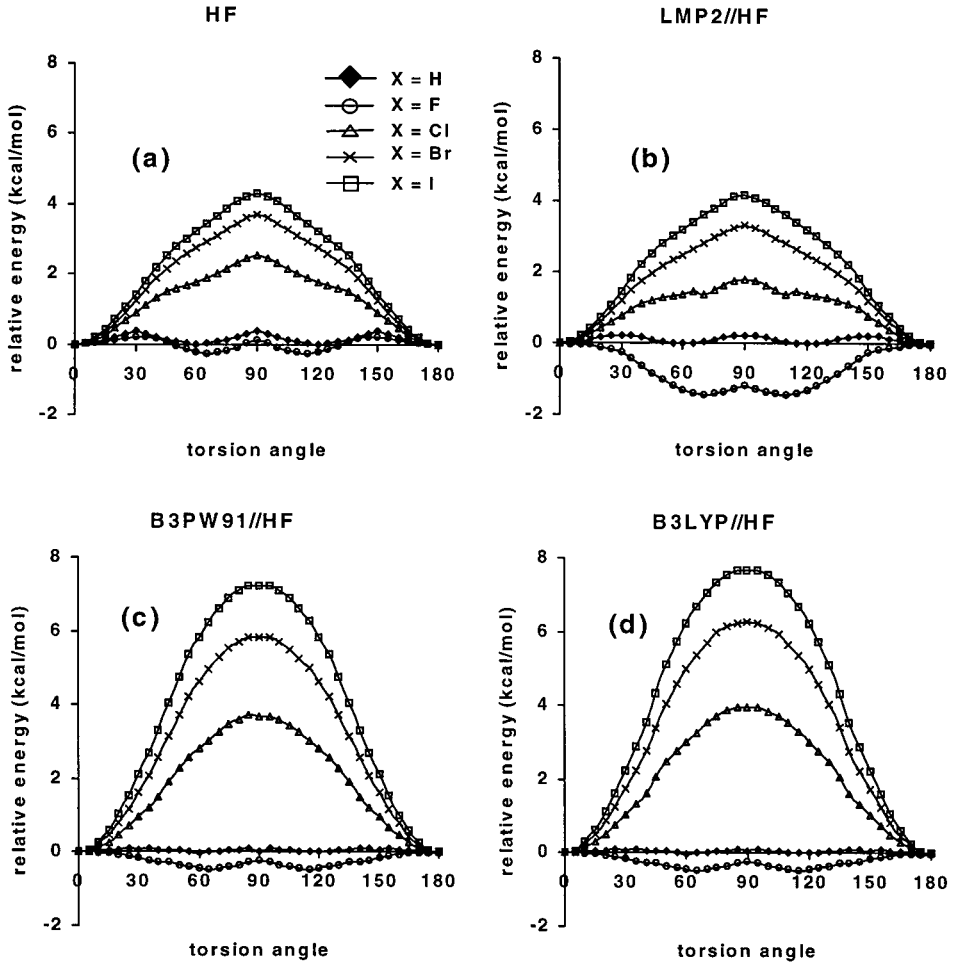

Figure 3. The energy of CH_2XCH_2 as a function of torsion angle (ω) (In these calculations the torsion angle was fixed and all structural parameters optimized.): (**a**) HF, (**b**) LMP2//HF, (**c**) B3PW91//HF, (**d**) B3LYP//HF.

reversal of Born−Oppenheimer potential energy surface was also observed in previous ab initio calculations[21] on the CH_2FCH_2 radical.

Early UHF calculations[42] with the 4-31G* basis set suggested that CH_2ClCH_2 has two minima and two transition states, just as for CH_2FCH_2. However, later UHF results[37] with the 6-31G* basis set showed that the CH_2ClCH_2 radical has only one minimum and one transition state for internal rotation about the C−C bond. Our results also support this conclusion.

For CH_2BrCH_2 and CH_2ICH_2, the potential energy curves for the internal rotation have not been previously reported. The general form for the rotational energy curves for the CH_2BrCH_2 and CH_2ICH_2 radicals are very similar to that of the CH_2ClCH_2 radical. They also have only one minimum at the anti conformation and only one saddle point at the IV rotamer. The LMP2//HF and HF calculations show comparable barriers while both DFT//HF methods (B3PW91//HF and B3LYP//HF) lead to barriers twice as high.

Compared with the C_2H_5 and CH_2FCH_2 radicals, the haloethyl radicals containing third-row or higher substituents have relatively high rotational barriers. The rotational barriers increase in the order of Cl, Br and I. The results calculated at LMP2 level were very close to those of LMP2//HF. Kochi and coworkers[15] estimated ~4 kcal/mol for the rotational barrier about C−C bond of the CH_2ClCH_2 radical from their ESR investigation. DFT calculations lead to results in good agreement with experiment (3.9 kcal/mol for B3PW91 and 3.5 kcal/mol for B3LYP) with larger errors for HF (2.6 kcal/mol), LMP2//HF (1.7 kcal/mol), and LMP2 (1.8 kcal/mol).

The structures optimized with the LMP2 method are very similar to those with HF while DFT geometries show considerable deviation from the LMP2 geometries. The DFT methods (B3PW91 and B3LYP) yield similar geometries.

The XCC bond angles in the haloethyl radicals at the asymmetric bridging minima in the rotational energy curve are only slightly less than the tetrahedral bond angle. At the anti conformations, the radical centers are slightly distorted from the perfectly planar form so that the singly occupied carbon 2p orbital is anti to the halogen.

An early INDO calculation[43] showed that CH_2ClCH_2 has the asymmetrically bridged structure. However, later ab initio studies[31−42] showed no evidence of asymmetric bridging.

Figure 4 displays the changes in the structural parameters as a function of the torsion angle. The behavior observed for C_2H_5 and CH_2FCH_2 radicals is quite different from that in the other haloethyl radicals. For C_2H_5 and CH_2FCH_2 radicals, the C−C bond length and C−X bond length are independent of the torsion angle while the X−C−C bond angle decreases from the I to IV rotamers. However, for the CH_2ClCH_2, CH_2BrCH_2, and CH_2ICH_2 radicals the C−C bond length increases and C−X bond length decreases from the I to the IV rotamer. The shape of the X−C−C bond angle as a function of the torsion angle has minima at the I and III conformations and maxima at II and IV conformations. The trends of C−C bond length and X−C−C bond angle might be explained solely by Pauli repulsion between the singly occupied carbon 2p orbital and the halogen doubly occupied orbitals. However, the trend in the C−X bond length is not rationalized by the same argument because it would

TABLE 2: Relative Energies (kcal/mol) of CH_2XCH_2 Radicals Calculated at Various Levels of Theory[a]

CH_3CH_2

Method	a-CH_3CH_2 (I)	te-CH_3CH_2 (IV)
HF	0	0.360 (−0.259)
LMP2//HF	0	0.167 (−0.452)
LMP2	0	0.193 (−0.426)
B3PW91	0	0.095 (−0.160)
B3LYP	0	0.098 (−0.167)

CH_2FCH_2

Method	a-CH_2FCH_2 (I)	g-CH_2FCH_2 (III)	tex-CH_2FCH_2 (IV)	teh-CH_2FCH_2 (II)
HF	0.253 (0.353)	0	0.413 (0.040)	0.465 (−0.255)
LMP2//HF	1.246 (1.346)	0	0.164 (−0.209)	1.015 (0.295)
LMP2	1.401 (1.501)	0	0.194 (−0.179)	converge to I
B3PW91	0.513 (0.797)	0	0.193 (−0.277)	converge to I
B3LYP	0.469 (0.753)	0	0.205 (−0.275)	converge to I

CH_2ClCH_2

Method	a-CH_2ClCH_2 (I)	b-CH_2ClCH_2	te-CH_2ClCH_2 (IV)
HF	−2.998 (−2.689)	0	−0.444 (−1.236)
LMP2//HF	−1.000 (−0.691)	0	0.673 (−0.122)
LMP2	−0.852 (−0.543)	0	0.942 (0.150)
B3PW91	−4.629 (−4.600)	0	−0.745 (−1.647)
B3LYP	−1.705 (−1.793)	0	2.786 (1.767)

CH_2BrCH_2

Method	a-CH_2BrCH_2 (I)	b-CH_2BrCH_2	te-CH_2BrCH_2 (IV)
HF	6.089 (6.071)	0	9.800 (8.599)
LMP2//HF	7.457 (7.439)	0	10.648 (9.447)
LMP2	7.583 (7.565)	0	10.519 (9.318)
B3PW91	0.991 (0.687)	0	7.310 (5.997)
B3LYP	converge to bridge	0	10.855 (9.522)

CH_2ICH_2

Method	a-CH_2ICH_2 (I)	b-CH_2ICH_2	te-CH_2ICH_2 (IV)
HF	12.281 (12.035)	0	16.591 (15.153)
LMP2//HF	12.219 (11.973)	0	16.272 (14.834)
LMP2	12.345 (12.099)	0	16.268 (14.830)
B3PW91	converge to bridge	0	12.343 (10.981)
B3LYP	converge to bridge	0	15.912 (14.481)

[a] The values in parentheses are corrected for the zero point energies. The anti conformer has a prefix of a- and the eclipsed form has a prefix of te-. The symmetrically bridged structure has a prefix of b-.

increase with the torsion angle to minimize the repulsion rather than decrease as observed in Figure 4.

On the basis of UMP2 calculation,[31] Guerra explained the unexpected trend of the C−X bond length in terms of the highly stabilizing interaction between the singly occupied carbon 2p orbital and σ^*(C−X) MO. This interaction (referred to as hyperconjugation) was studied extensively by Bernardi and coworkers.[24,32,39] They performed fragment interaction analysis of the UHF calculations and concluded that the contribution of hyperconjugation between the singly occupied carbon 2p orbital and σ^*(C−X) MO is dominant in determining conformational preference in the β-chloroethyl radical. The trends of the relative energies and other structural parameters are also consistent with this hyperconjugation. Figure 5 shows a schematic of the singly occupied highest molecular orbital (SOMO) we find for rotamers I and IV. The hyperconjugation is maximum in the anti conformation (rotamer I) and decreases with increasing torsion angle. The SOMO of rotamer I results from hyperconjugation between the carbon 2p orbital and the σ^*(C−X) MO. In contrast, the SOMO of IV has hyperconjugation between the 2p orbital and σ^*(C−H) MO, which is much weaker. Thus, the IV rotamer has the maximum energy due to the absence of this stabilizing hyperconjugation between the carbon 2p orbital and the σ^*-(C−X) MO. Since hyperconjugation enhances the C−C double bond character and weakens the C−X bond, the anti conformer has the minimum C−C bond length and the maximum C−X bond length.

By means of the electron transmission spectroscopy on *tert*-butyl halides $(CH_3)_3CX$, Modeli et al.[64] observed that the σ^*-(C−X) MOs lie low in energy only for X in the Br, I, and higher rows. They reproduced these experimental results using MXSα calculations (an approximation to the LDA approximation of DFT). We also examined the SOMO and LUMO energies for CH_2XCH_2 radicals. Table 4 lists the SOMO and LUMO energies and also the differences for the rotamer IV calculated at various levels of theory as discussed above. The rotamer IV is expected to have the least hyperconjugation. It is clear that the LUMO energies are very low for X = Cl, Br, and I compared to X = H and F. Especially, the LUMO energies calculated with DFT methods seem to emphasize these trends. This might explain the higher rotational barriers (energy difference between I and IV) calculated with the DFT methods compared to the LMP2 results. The more electronegative halogen (F) disfavors hyperconjugation by raising the energy of the σ^*(C−X) MO. This is also consistent with the magnitudes of the changes in the structural parameters, which increase in the order Cl, Br, and I. From Table 3, we see that the C−C bond lengths of rotamer I dramatically decrease from X = F to X = I while rotamer IV

TABLE 3: Optimized Structural Parameters of β-Substituted Ethyl Radicals ($C_\beta H_2X\text{-}C_\alpha H_2$)[a]

(a) HF level

	X = H		X = F				X = Cl		X = Br		X = I	
	I	IV*	I	II*	III	IV*	I	IV*	I	IV*	I	IV*
$r(C_\alpha-C_\beta)$	1.498	1.497	1.490	1.489	1.489	1.489	1.474	1.488	1.467	1.488	1.464	1.490
$r(C_\beta-X)$	1.090	1.085	1.379	1.376	1.371	1.370	1.875	1.836	2.062	2.009	2.246	2.181
$\angle XC_\beta C_\alpha$	111.7	111.4	110.7	110.5	110.0	110.0	110.6	111.5	110.6	112.0	111.3	113.1
$r(C_\beta-H_{3\beta})$	1.086	1.088	1.083	1.086	1.088	1.087	1.077	1.081	1.076	1.080	1.077	1.081
$r(C_\beta-H_{4\beta})$	1.086	1.089	1.083	1.083	1.085	1.087	1.077	1.081	1.076	1.080	1.077	1.081
$\angle H_{3\beta}CC$	111.3	111.5	111.2	111.5	111.8	111.6	113.4	112.8	114.1	113.0	114.1	112.7
$\angle H_{4\beta}CC$	111.3	111.6	111.3	111.4	111.3	111.6	113.4	112.7	114.1	113.0	114.1	112.7
$\angle H_{3\beta}CH_{4\beta}$	108.0	106.8	108.8	108.5	108.1	107.8	110.7	109.0	111.3	109.2	111.2	108.7
$r(C_\alpha-H_{1\alpha})$	1.075	1.074	1.074	1.072	1.074	1.073	1.073	1.074	1.073	1.074	1.073	1.075
$r(C_\alpha-H_{2\alpha})$	1.075	1.072	1.074	1.073	1.074	1.071	1.073	1.070	1.073	1.070	1.073	1.070
$\angle H_{1\alpha}CC$	119.7	120.5	119.6	121.5	119.5	120.0	119.4	118.4	119.6	118.1	119.8	118.0
$\angle H_{2\alpha}CC$	119.7	121.6	119.6	119.4	118.6	119.9	119.4	121.6	119.6	122.2	119.8	122.7
θ	78.5	90.1	79.5	87.2	101.9	89.9	80.0	90.0	80.7	90.0	81.2	90.0
ω	0.0	90.0	0.0	34.6	65.6	90.0	0.0	90.0	0.0	90.0	0.0	90.0

(b) LMP2 level

	X = H		X = F				X = Cl		X = Br		X = I	
	I	IV*	I*	II	III	IV*	I	IV*	I	IV*	I	IV*
$r(C_\alpha-C_\beta)$	1.497	1.496	1.496		1.489	1.489	1.481	1.484	1.472	1.485	1.468	1.491
$r(C_\beta-X)$	1.096	1.089	1.405		1.399	1.398	1.855	1.822	2.035	1.986	2.212	2.153
$\angle XC_\beta C_\alpha$	111.6	111.4	111.3		110.0	109.8	111.6	111.4	111.3	112.5	111.8	112.5
$r(C_\beta-H_{3\beta})$	1.090	1.094	1.091		1.097	1.096	1.086	1.091	1.086	1.090	1.086	1.091
$r(C_\beta-H_{4\beta})$	1.090	1.094	1.090		1.093	1.095	1.086	1.091	1.086	1.091	1.086	1.090
$\angle H_{3\beta}CC$	111.3	111.4	110.6		111.5	111.7	111.2	112.2	112.8	111.8	112.8	111.7
$\angle H_{4\beta}CC$	111.4	111.5	110.9		111.3	111.8	112.3	111.4	112.9	112.0	112.9	111.8
$\angle H_{3\beta}CH_{4\beta}$	108.1	106.7	107.9		107.9	107.6	109.7	108.0	110.1	108.1	109.9	107.6
$r(C_\alpha-H_{1\alpha})$	1.080	1.079	1.079		1.080	1.078	1.079	1.081	1.080	1.087	1.080	1.082
$r(C_\alpha-H_{2\alpha})$	1.080	1.078	1.079		1.079	1.077	1.079	1.077	1.080	1.078	1.080	1.077
$\angle H_{1\alpha}CC$	120.2	120.5	120.5		119.2	120.1	119.6	118.7	119.8	116.4	119.9	118.4
$\angle H_{2\alpha}CC$	120.1	121.6	119.8		118.8	119.7	119.8	121.7	119.9	120.9	120.0	122.5
θ	80.7	91.2	82.5		100.4	90.0	80.7	90.8	81.0	101.4	80.9	91.0
ω	0.0	90.0	0.0		69.5	90.0	0.0	90.0	0.0	78.0	0.0	90.0

(c) B3PW91 level of DFT

	X = H		X = F				X = Cl		X = Br		X = I	
	I	IV*	I*	II	III	IV*	I	IV*	I	IV*	I	IV*
$r(C_\alpha-C_\beta)$	1.485	1.485	1.482		1.478	1.478	1.451	1.476	1.427	1.476		1.477
$r(C_\beta-X)$	1.103	1.094	1.404		1.387	1.384	1.931	1.843	2.170	2.014		2.191
$\angle XC_\beta C_\alpha$	112.1	111.9	110.8		111.0	111.0	109.7	112.1	108.2	112.5		113.4
$r(C_\beta-H_{3\beta})$	1.096	1.100	1.096		1.105	1.104	1.089	1.096	1.087	1.096		1.094
$r(C_\beta-H_{4\beta})$	1.096	1.100	1.096		1.100	1.104	1.089	1.096	1.087	1.096		1.096
$\angle H_{3\beta}CC$	111.8	111.9	111.3		111.6	111.5	114.5	112.9	116.4	113.2		112.9
$\angle H_{4\beta}CC$	111.8	111.9	111.3		111.2	111.5	114.5	112.8	116.4	113.2		113.1
$\angle H_{3\beta}CH_{4\beta}$	108.0	105.8	108.5		106.9	106.5	114.4	107.7	113.1	108.0		107.8
$r(C_\alpha-H_{1\alpha})$	1.085	1.085	1.085		1.084	1.084	1.084	1.085	1.084	1.086		1.087
$r(C_\alpha-H_{2\alpha})$	1.085	1.084	1.085		1.084	1.082	1.084	1.082	1.084	1.081		1.083
$\angle H_{1\alpha}CC$	120.8	120.6	120.5		120.2	120.2	120.4	118.6	120.6	118.3		117.6
$\angle H_{2\alpha}CC$	120.8	121.7	120.5		119.5	120.1	120.4	121.8	120.6	122.4		122.2
θ	84.3	90.0	83.3		96.5	89.6	83.9	90.0	85.0	90.0		98.5
ω	0.0	90.0	0.0		64.4	90.0	0.0	90.0	0.0	90.0		81.5

(d) B3LYP level of DFT

	X = H		X = F				X = Cl		X = Br		X = I	
	I	IV*	I*	II	III	IV*	I	IV*	I	IV*	I	IV*
$r(C_\alpha-C_\beta)$	1.489	1.489	1.484		1.480	1.481	1.447	1.479		1.479		1.480
$r(C_\beta-X)$	1.104	1.094	1.411		1.393	1.390	1.970	1.858		2.030		2.204
$\angle XC_\beta C_\alpha$	112.1	111.9	110.6		110.8	110.8	109.2	112.1		112.5		113.5
$r(C_\beta-H_{3\beta})$	1.096	1.101	1.096		1.105	1.104	1.087	1.096		1.095		1.095
$r(C_\beta-H_{4\beta})$	1.096	1.101	1.096		1.100	1.104	1.087	1.096		1.095		1.095
$\angle H_{3\beta}CC$	111.8	112.0	111.4		111.8	111.5	115.2	113.0		112.4		113.1
$\angle H_{4\beta}CC$	111.8	112.0	111.4		111.3	111.6	115.2	113.0		113.4		113.1
$\angle H_{3\beta}CH_{4\beta}$	108.1	105.7	108.7		106.9	106.6	112.0	107.8		108.1		107.7
$r(C_\alpha-H_{1\alpha})$	1.085	1.083	1.084		1.084	1.083	1.084	1.085		1.086		1.081
$r(C_\alpha-H_{2\alpha})$	1.085	1.084	1.084		1.084	1.082	1.084	1.081		1.081		1.086
$\angle H_{1\alpha}CC$	120.8	121.7	120.5		120.2	120.2	120.5	118.5		118.2		123.0
$\angle H_{2\alpha}CC$	120.8	120.6	120.5		119.5	120.0	120.5	121.8		122.5		118.1
θ	84.3	90.0	83.3		91.0	89.5	84.1	90.1		90.0		90.1
ω	0.0	90.0	0.0		69.5	90.0	0.0	90.0		90.0		90.0

[a] The bond lengths are in Å and the angles are in degrees. The blanks indicate that the corresponding structure cannot be located either in a minimum or in a saddle point.

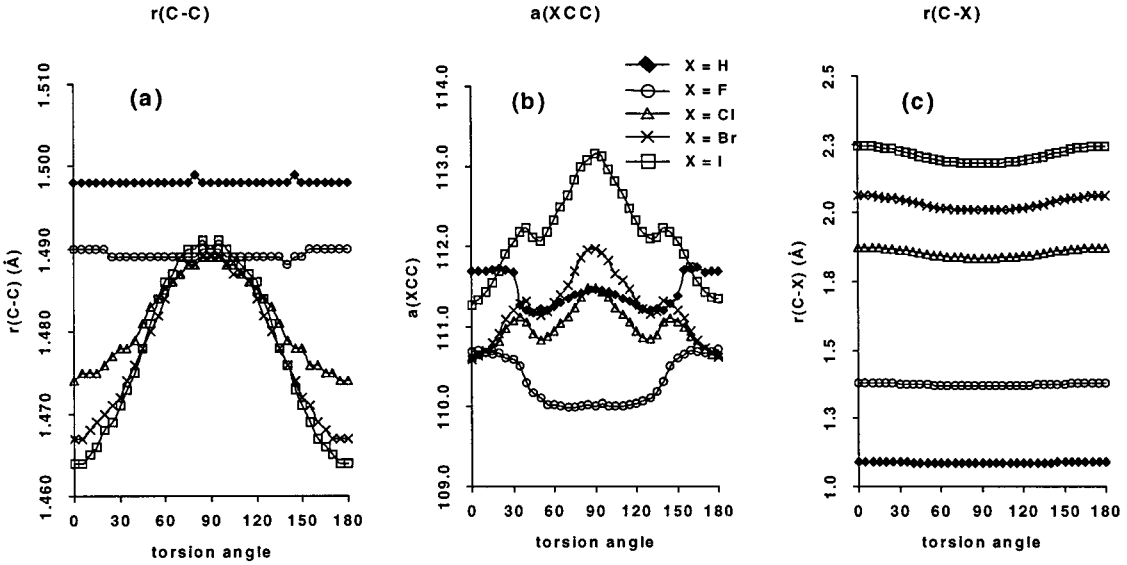

Figure 4. The geometric parameters optimized as a function of torsion angle (ω) with the HF method: (**a**) C−C bond length (Å), (**b**) X−C−C angle (deg), (**c**) C-X bond length (Å).

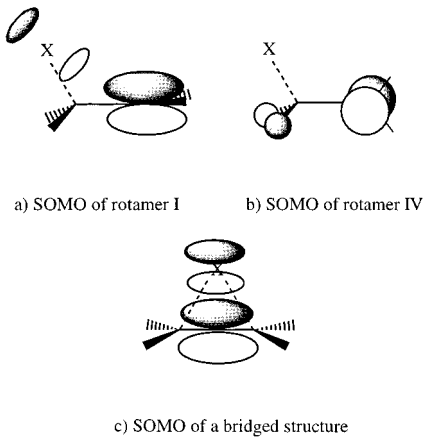

Figure 5. A schematic representations of the singly occupied highest molecular orbital (SOMO) of CH_2XCH_2 radical (X = Cl, Br, and I): (**a**) rotamer I, (**b**) rotamer IV, and (**c**) symmetrically bridged structure.

shows little change. This observation is also consistent with the hyperconjugation explanation.

4.2. Bridged Structures. At all levels of theory in this study, the radicals with X = Cl, Br, and I lead to symmetrically bridged minima with no imaginary frequency. For the CH_2ClCH_2 radical, all methods predict that the bridged structure is less stable than the anti conformer. In contrast, the bridged structures are the global minima for CH_2BrCH_2 and CH_2ICH_2 radicals at all levels of calculation. At the LMP2 level, the bridged form is more stable than the anti form by more than 7 kcal/mol for CH_2BrCH_2 and 12 kcal/mol for CH_2ICH_2. The B3PW91 and B3LYP methods indicate that the anti conformation of the CH_2ICH_2 radical is not a local energy minimum. Also, the anti CH_2BrCH_2 radical optimized with B3LYP converged to the bridged structure. The calculated total energies and the relative energies for the symmetrically bridged structures at various levels of theory are presented in Tables 1 and 2, respectively. The optimized structural parameters calculated at various levels of theory are also given in Table 5, and Table 6 lists the vibrational frequencies and assignments.

The symmetrically bridged conformation of CH_2ClCH_2 was studied previously. Fossey and Nedelec[26] used UHF with the STO-3G basis set to study the 1,2-migrations observed in many free radical reactions. They reported that the bridged CH_2ClCH_2 radical is 53 kcal/mol higher than the anti structure, but still stable to the dissociation. However, Hoz et al.[40] studied 1,2-rearrangement of CH_2ClCH_2 using the active space multiconfiguration SCF method and reported that the bridged structure is above the C_2H_4 + Cl dissociation limit. In contrast, Engels et al.[38] reported MRD-CI calculations indicating that the symmetrically bridged structure is stable with respect to the dissociation reaction. Their bridged conformation corresponds to the transition state for the shuttle motion. From unrestricted MP2 calculations, Guerra[31] also reported that the $^2A_1$ state of the symmetrically bridged CH_2ClCH_2 radical is below the dissociation limit while the $^2B_2$ state is dissociative without a minimum and lies above the $^2A_1$ state. The vibrational frequencies calculated for the symmetrically bridged CH_2ClCH_2 radical are all real in our calculation, indicating that it is located at a local minimum rather than a saddle point. Engels et al. studied also CH_2BrCH_2 radical[35] where they reported that the bridged

TABLE 4: SOMO and LUMO Energy (Hartrees) of the IV Rotamer of CH_2XCH_2

	SOMO	LUMO	LUMO−SOMO
		HF	
C_2H_5	−0.17460	0.25865	0.43325
CH_2FCH_2	−0.18469	0.25851	0.44320
CH_2ClCH_2	−0.19116	0.18879	0.37995
CH_2BrCH_2	−0.19098	0.14300	0.33398
CH_2ICH2	−0.18978	0.10579	0.29557
		LMP2	
C_2H_5	−0.17462	0.25781	0.43243
CH_2FCH_2	−0.18536	0.25583	0.44119
CH_2ClCH_2	−0.19032	0.19282	0.38314
CH_2BrCH_2	−0.19497	0.14994	0.34491
CH_2ICH_2	−0.18872	0.11009	0.29881
		B3PW91	
C_2H_5	−0.10000	0.12519	0.22519
CH_2FCH_2	−0.10881	0.10513	0.21394
CH_2ClCH_2	−0.11457	0.01644	0.13101
CH_2BrCH_2	−0.11455	−0.01626	0.09829
CH_2ICH2	−0.11541	−0.03897	0.07644
		B3LYP	
C_2H_5	−0.09759	0.11733	0.21492
CH_2FCH_2	−0.10658	0.10192	0.20850
CH_2ClCH_2	−0.11213	0.01378	0.12591
CH_2BrCH_2	−0.11208	−0.01880	0.09328
CH_2ICH_2	−0.11132	−0.04026	0.07106

TABLE 5: Optimized Structure of the Bridged Radicals at Various Levels of Theory[a]

	HF	LMP2	B3PW91	B3LYP
		C_2H_4		
r(C−X)				
∠CXC				
r(C−C)	1.317	1.336	1.329	1.330
r(C−H)	1.077	1.082	1.087	1.087
∠HCC	121.7	121.5	121.8	121.8
		CH_2ClCH_2		
r(C−X)	3.515	3.500	2.660	2.705
		3.562		
∠CXC	21.6	21.9	29.5	29.0
r(C−C)	1.319	1.340	1.355	1.354
r(C−H)	1.076	1.082	1.085	1.085
∠HCC	121.7	121.4	121.4	121.5
		CH_2BrCH_2		
r(C−X)	3.620	3.704	2.829	2.889
		3.562		
∠CXC	21.0	20.7	27.7	27.7
r(C−C)	1.319	1.340	1.352	1.352
r(C−H)	1.076	1.082	1.086	1.085
∠HCC	121.7	121.4	121.5	121.5
		CH_2ICH_2		
r(C−X)	3.894	4.028	3.079	3.159
		4.042		
∠CXC	19.5	19.1	25.3	25.1
r(C−C)	1.319	1.339	1.348	1.347
r(C−H)	1.076	1.082	1.086	1.086
∠HCC	121.7	121.5	121.5	121.6

[a] The bond lengths are in Å and the angles are in degrees.

form has a local minimum. But they did not fully optimize the geometries (due to the high computational cost for obtaining a whole potential energy hypersurface). While their results indicate that the symmetrically bridged structure is less stable than the anti conformer, the symmetrically bridged form is a global minimum in our calculation.

The C_2H_4 moiety of the bridged structure has almost same structure as the free C_2H_4 molecule except that the C−C bond lengths are elongated, reflecting the interaction between the halogen atom and the π orbital of the C_2H_4 moiety. However, the C−C bond length of the bridged structure is much closer to that of double bond character than that of the single bond. In Table 6, the vibrational frequency showing the most apparent change from C_2H_4 to the bridged CH_2XCH_2 is the C−C stretch mode. Due to the weakened C−C bond in the bridged CH_2XCH_2, the vibrational frequency for the C−C stretch is reduced but still relatively close to that of C_2H_4 compared to anti form of CH_2XCH_2. The SOMO of the symmetrically bridged form is represented schematically in Figure 5. This SOMO is the result of the interaction between the halogen p orbital and the π orbital of the C_2H_4 moiety. The C−X bond length in the bridged structure is about 30% longer than that of anti conformation due to the relatively weak interaction between halogen and carbon atoms. Engels et al.[38] reported a C−Cl bond length of 2.98 Å for the symmetrically bridged conformation of the CH_2ClCH_2 radical. Our HF and LMP2 calculations give higher values and the DFT methods give slightly lower values. Actually, our DFT values are very close to 2.58 Å by Guerra[31] and 2.68 Å reported by Fossey and Nedelec.[26] The C−Br internuclear distances calculated with DFT for CH_2BrCH_2 radical are also very close to the 2.98 Å from Engels et al.[35] The geometries optimized with the LMP2 method are slightly asymmetric. However, the amount of deviation from the perfectly symmetric form is too small to be attributed to the asymmetrically bridged radical. The DFT methods describe the symmetrically bridged structures better than HF and LMP2 methods.

4.3. Shuttle Motion and Dissociation. To study the shuttle motion and the dissociation mechanism, the geometries were optimized as a function of the position of halogen atom with the B3PW91 method. The resulting potential energy surfaces for CH_2ClCH_2, CH_2BrCH_2, and CH_2ICH_2 are depicted in Figures 6, 7, and 8, respectively. In the calculation, the halogen atom was confined in the X−C−C plane bisecting the H−C−H angle.

The contour maps clearly show the relative stability of the anti conformer and the symmetrically bridged structure. For the CH_2ClCH_2 radical, the global minimum corresponds to the anti conformer while the symmetric conformation corresponds to a local minimum. The region around the symmetric conformation is very flat along the C−C axis leading to the lowest vibrational frequency of only 33 cm^{-1}. The barrier from the symmetrically bridged form to the anti conformation is almost zero. The relative stability is reversed in the CH_2BrCH_2 radical, and the anti conformation is no longer stable for the CH_2ICH_2 radical. The potential energy surfaces for the region of the symmetrically bridged conformations are bounded and also very flat. Therefore, we can expect high amplitude shuttle motion around the symmetric conformation especially for the CH_2BrCH_2 and CH_2ICH_2 radicals. The shuttle motion should be considered as a rocking motion of the ethylene moiety around the heavy halogen atom rather than the direct movement of the halogen atom. These shuttle motions can be visualized by examining the vibrational

TABLE 6: Vibrational Frequencies of CH_2XCH_2 Radicals and C_2H_4 Calculated with DFT Methods (B3PW91 and B3LYP)[a]

	C_{2v}	b-CH_2ClCH_2	b-CH_2BrCH_2	b-CH_2ICH_2	D_{2h}	C_2H_4		C_s	a-CH_2ClCH_2	a-CH_2BrCH_2
cis CH stretch	B_1	3300 (3286[b])	3294 (3280)	3288 (3273)	B_{2u}	3258 (3244)	asym CH stretch of $^{\bullet}CH_2$	A″	3301 (3287)	3300
trans CH stretch	A_2	3278 (3263)	3272 (3257)	3265 (3250)	B_{3g}	3234 (3219)	asym CH stretch of XCH_2	A″	3222 (3220)	3249
symm CH stretch	A_1	3192 (3182)	3188 (3178)	3184 (3174)	A_g	3170 (3159)	symm CH stretch of $^{\bullet}CH_2$	A′	3188 (3177)	3187
anti CH stretch	B_2	3185 (3176)	3180 (3171)	3176 (3166)	B_{1u}	3154 (3145)	symm CH stretch of XCH_2	A′	3142 (3141)	3162
CC stretch	A_1	1639 (1641)	1644 (1647)	1654 (1657)	A_g	1720 (1717)	CC stretch	A′	1132 (1127)	1103
anti HCH bend	B_2	1470 (1479)	1471 (1481)	1471 (1481)	B_{1u}	1471 (1480)	anti HCH bend	A′	1465 (1473)	1463
symm HCH bend	A_1	1358 (1360)	1361 (1362)	1365 (1367)	A_g	1385 (1387)	symm HCH bend	A′	1512 (1520)	1521
anti HCH wag	A_2	1234 (1239)	1234 (1240)	1234 (1240)	B_{3g}	1233 (1239)	anti HCH wag	A″	1252 (1250)	1241
H_2C-CH_2 twist	A_2	961 (965)	988 (988)	1009 (1005)	A_u	1070 (1071)	XCH_2 scissor + $^{\bullet}CH_2$ wag	A″	1052 (1039)	998
symm out of plane	A_1	993 (993)	997 (996)	998 (994)	B_{3u}	976 (978)	CH_2 rock of $^{\bullet}CH_2$	A′	688 (705)	750
anti out of plane	B_2	971 (973)	975 (974)	977 (974)	B_{2g}	964 (963)	CH_2 rock of XCH_2	A′	1229 (1210)	1178
symm HCH wag	B_1	829 (832)	828 (832)	827 (831)	B_{2u}	825 (828)	symm HCH wag	A″	781 (784)	780
shuttle perp. to CC	B_1	323 (300)	327 (293)	300 (246)			torsion	A″	277 (299)	356
X−(C_2H_4) stretch	A_1	218 (212)	178 (166)	141 (126)			$^{\bullet}CH_2$ rock + XCH_2 rock	A′	466 (403)	232
shuttle along CC	B_2	33 (86)	97 (96)	111 (90)			XCC bend	A′	300 (291)	298

[a] The anti conformer has a prefix of a- and the symmetrically bridged structure has a prefix of b-. Symmetry species in each row are symmetrically correlated. Unscaled values and represented in cm^{-1}. [b] B3LYP values are presented in parentheses.

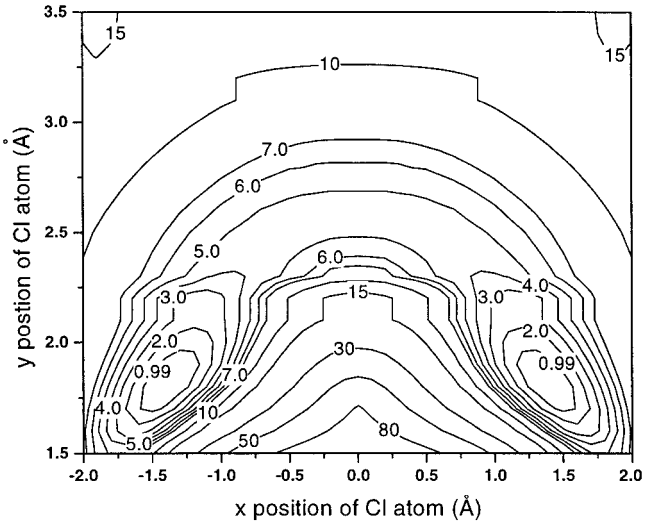

Figure 6. The contour map constructed for CH_2ClCH_2 with the B3PW91 method. The position of halogen atom is referenced to the middle point of two carbon atoms. The zero of energy corresponds to the global minimum (anti rotamer (I)).

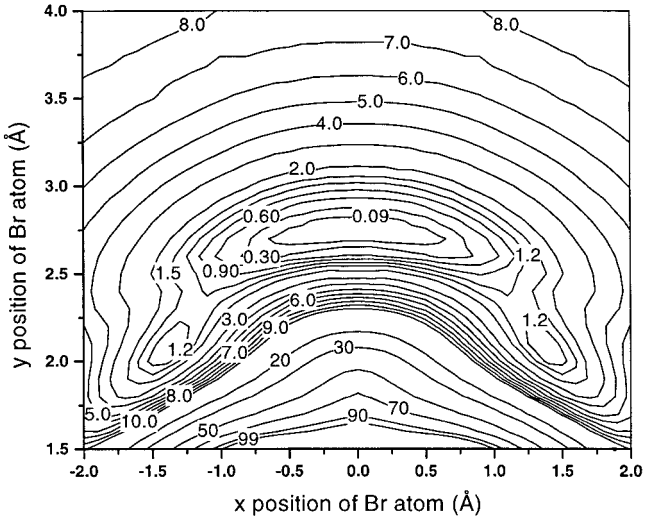

Figure 7. The contour map constructed for CH_2BrCH_2 with the B3PW91 method. The position of halogen atom is referenced to the middle point of two carbon atoms. The zero of energy corresponds to the global minimum (symmetrically bridged form).

modes of the bridged radicals. The lowest vibrational frequency corresponds to the rocking motion of the C_2H_4 moiety along C−C axis, and the second lowest one corresponds to the X−(C_2H_4) stretch motion perpendicular to the C−C axis. The rocking motion out of the X−C−C plane bisecting the H−C−H angle is the third lowest frequency. The rocking motion of the

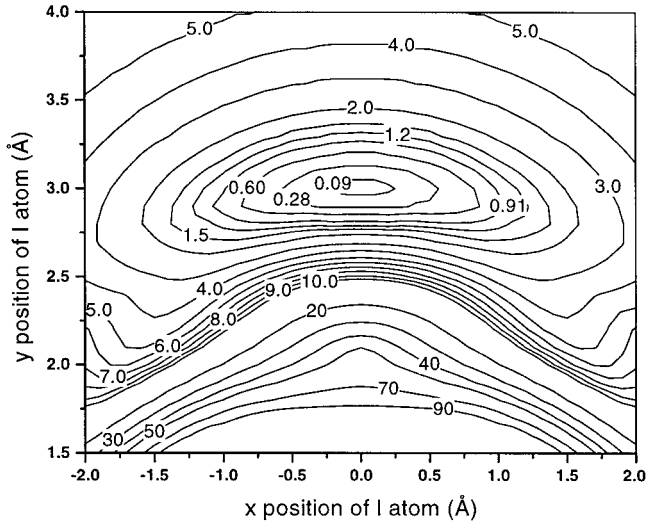

Figure 8. The contour map constructed for CH_2ICH_2 with the B3PW91 method. The position of halogen atom is referenced to the middle point of two carbon atoms. The zero of energy corresponds to the global minimum (symmetrically bridged form).

C_2H_4 moiety along C−C axis is conceptually similar to the dynamic shuttle motion proposed by Skell and co-workers,[47] except that the symmetrically bridged conformation actually corresponds to a minimum rather than a saddle point. In other word, it is more compatible with the shuttle motion of Engels and Peyerimhoff.[35]

It is evident from the results that the bridged structures should play an important role in the dissociation process of CH_2XCH_2 for the cases of X = Cl, Br, and I. In particular, the bridged structures should be the dominant conformers for the CH_2BrCH_2 and CH_2ICH_2 radicals. This suggests that Skell's hypothesis of symmetric bridging[7,48] *can* explain the stereochemical control of the CH_2BrCH_2 and CH_2ICH_2 radicals. Engels and Peyerimhoff also proposed that the symmetrically bridged radical plays an important role in the dissociation process of the CH_2ClCH_2 radical.[38] They suggested that the symmetrically bridged structure can be an intermediate species along the dissociation process.

The DFT methods lead to energetics considerably different than that of the HF and LMP2 methods. Table 7 lists the dissociation energies for the C−X bond cleavage. The global minimum of the radical was taken for obtaining the dissociation energy. Correcting for zero point energy, we see that for X = H DFT is high by 3−4 kcal/mol, LMP2 is low by 3−4 kcal/mol, and HF is within 1 kcal/mol of the experimental data. For X = F, DFT is within the range of experimental uncertainty, while LMP2 is low by at least 3 kcal/mol and HF is low by 22 kcal/mol (50%). For X = Cl, DFT is low by 3−6 kcal/mol,

TABLE 7: Dissociation Energy (kcal/mol) for $CH_2XCH_2^{\bullet} \rightarrow CH_2{=}CH_2 + X$ Reaction[a]

method	X = H	X = F	X = Cl	X = Br	X = I
HF	40.28 (35.22)	24.48 (23.15)	3.90 (2.47)	0.93 (0.58)	0.93 (−0.58)[e]
LMP2//HF	37.21 (32.15)	43.45 (42.12)	0.24 (−1.19)	−0.89 (−1.24)	−0.88 (−1.23)[e]
LMP2	36.94 (31.88)	43.62 (42.29)	0.12 (−1.31)	−0.85 (−1.20)	−0.83 (−1.18)[e]
B3PW91	44.40 (39.18)	49.94 (48.77)	15.67 (14.90)	8.66 (7.75)	5.88 (5.12)[e]
B3LYP	43.69 (38.52)	48.78 (47.68)	12.23 (11.54)	8.02 (7.29)	5.23 (4.61)[e]
experiment	35.5 ± 1.0[a]	45−50[b]	18.2 ± 2.2[c]	8.4 ± 2.2[c]	−10.1 ± 1.6[d]

[a] The values in the parenthesis are corrected for the zero point energies. Estimated using $\Delta H_{f,300K}(C_2H_5) = 28.0 \pm 1.0$ kcal/mol,[68] and $\Delta H_{f,0K}(C_2H_4)$ and $\Delta H_{f,0K}(H)$ from JANAF.[69] The thermal enthalpy is corrected for 0 K. [b] Estimated by Schlegel et al.[70] [c] Estimated using $\Delta H_f(CH_2ClCH_2^{\bullet})$ from Ref. 71 and $\Delta H_f(C_2H_4)$ and $\Delta H_f(X)$ from the JANAF table.[69] The thermal enthalpy is corrected for 0 K. The estimated value for CH_2ClCH_2 is close to the 21.3 kcal/mol estimated in different way.[72] [d] Estimated assuming that $D_0(CH_2XCH_2-H) = D_0(CH_3CH_2-H)$. The $\Delta H_f(C_2H_4)$, $\Delta H_f(CH_2XCH_3)$, $\Delta H_f(H)$, and $\Delta H_f(X)$ are taken from the JANAF table.[69] [e] The calculated bond energy should be decreased by ∼8 kcal/mol to reflect the spin−orbit coupling in the case of X = I.

while LMP is low by ~19 kcal/mol (over 100%) and HF is low by 14 kcal/mol. For X = Br, DFT is within the experimental range, while LMP2 is low by 9 kcal/mol (over 100%) and HF is low by 7 kcal/mol. Including a correction for spin−orbit interaction in the I atom, we see that for X = I, DFT is high by 7 kcal/mol while LMP2 is within the experimental range. It should be noted that the experimental values for X = Cl, Br, and I are obtained assuming that $D^0(CH_2XCH_2-H) = D^0(CH_3-CH_2-H)$. Overall the DFT methods lead to the most accurate description for dissociation of the radicals.

5.0. Conclusion

To elucidate the origin of the stereoselectivity observed in halogenation reactions of alkenes, we studied the structures and potential energy surface of haloethyl radicals (CH_2XCH_2, X = F, Cl, Br, I) using first principles quantum mechanics. We find that radicals with X = Br and I are significantly different than the cases of X = F and Cl. Thus, the CH_2FCH_2 radical prefers the gauche conformation in the rotational potential energy surface while all other haloethyl radicals have the global minima at the anti conformation, which is stabilized by the donation of electron density from the singly occupied carbon 2p orbital to the σ^*(C−X) MO. The rotational barriers and the behaviors of the structural parameters along the rotational potential energy surface are highly consistent with this hyperconjugative interaction. The DFT results do much better at describing the dissociation process and the bridged radicals than the HF and LMP2 methods.

We conclude that the symmetrically bridged structure should play an important role in the dissociation processes of the $CH_2ClCH_2^\bullet$, $CH_2BrCH_2^\bullet$, and $CH_2ICH_2^\bullet$ radicals. The $CH_2BrCH_2^\bullet$ and $CH_2ICH_2^\bullet$ radicals strongly prefer the symmetric bridging conformation, which explains the stereoselective control of these radicals in the radical chemistry.

There has not yet been experimental observation of the CH_2BrCH_2 and CH_2ICH_2 radicals. Lee and co-workers[65] reported that stable CH_2BrCH_2 could not be unambiguously observed in their photofragment translational spectroscopy experiment. However, a very similar species, namely CF_2ICF_2 radical, was observed recently by means of ultrafast electron diffraction techniques.[66] The structure of the short-lived (~17 ps lifetime) CF_2ICF_2 radical was consistent with a mixture of anti and gauche conformers rather than the symmetrically bridged structure. The experimental observation is consistent with our ab initio calculations.[66,67] In addition, the Zewail lab is using the ultrafast electron diffraction techniques to investigate the molecular structures of the CH_2BrCH_2 and CH_2ICH_2 radicals.[73]

Acknowledgment. This research was funded (W.A.G.) by the NSF (CHE 95-12279), and a grant (A.Z.) from the Air Force Office of Scientific Research and the Office of Naval Research. The facilities of the MSC are also supported by grants from DOE-ASCI, BP Chemical, ARO-MURI, ARO-DURIP, Owens-Corning, Exxon, Chevron Corp., Dow Chemical, Avery Dennison, Beckman Institute, and Asahi Chemical. H.I. is grateful to Dr. S. Hwang and J. Kua for their technical help.

References and Notes

(1) Kochi, J. K. *Free Radicals*; John Wiley & Sons: New York, 1973; Vol. II.
(2) Beckwith, A. L. J.; Ingold, K. U. *Free-Radical Rearrangements*; Mayo, P. d., Ed.; Academic Press: New York, 1980.
(3) Kerr, J. A. *Handbook of Bimolecular and Termolecular Gas Reactions*; CRC Press: Boca Raton, FL, 1981; Vol. I.
(4) Fossey, J.; Lefort, D.; Sorba, J. *Free Radicals in Organic Chemistry*; John Wiley & Sons: New York, 1995.
(5) Goering, H. L.; Abell, P. I.; Aycock, B. F. *J. Am. Chem. Soc.* **1952**, *74*, 3588.
(6) Thaler, W. *J. Am. Chem. Soc.* **1963**, *85*, 2607.
(7) Skell, P. S.; Tuleen, D. L.; Readio, P. D. *J. Am. Chem. Soc.* **1963**, *85*, 2849.
(8) Tanner, D. D.; Darwish, D.; Mosher, M. W.; Bunce, N. J. *J. Am. Chem. Soc.* **1969**, *91*, 7398.
(9) Traynham, J. G.; Lee, Y.-S. *J. Am. Chem. Soc.* **1974**, *96*, 3590.
(10) Edge, D. J.; Kochi, J. K. *J. Am. Chem. Soc.* **1972**, *94*, 6485.
(11) Kawamura, T.; Edge, D. J.; Kochi, J. K. *J. Am. Chem. Soc.* **1972**, *94*, 1752.
(12) Chen, K. S.; Krusic, P. J.; Meakin, P.; Kochi, J. K. *J. Phys. Chem.* **1974**, *78*, 2014.
(13) Bowles, A. J.; Hudson, A.; Jackson, R. A. *Chem. Phys. Lett.* **1970**, *5*, 552.
(14) Elson, I. H.; Chen, K. S.; Kochi, J. K. *Chem. Phys. Lett.* **1973**, *21*, 72.
(15) Chen, K. S.; Elson, I. H.; Kochi, J. K. *J. Am. Chem. Soc.* **1973**, *95*, 5341.
(16) Cooper, J.; Hudson, A.; Jackson, R. A. *Tetrahedron Lett.* **1973**, 831.
(17) Krusic, P. J.; Bingham, R. C. *J. Am. Chem. Soc.* **1976**, *98*, 230.
(18) Parson, J. M.; Lee, Y. T. *J. Chem. Phys.* **1972**, *56*, 4658.
(19) Farrar, J. M.; Lee, Y. T. *J. Chem. Phys.* **1976**, *65*, 1414.
(20) Jacox, M. E. *Chem. Phys.* **1981**, *58*, 289.
(21) Chen, Y.; Rauk, A.; Tschuikow-Roux, E. *J. Chem. Phys.* **1990**, *93*, 6620.
(22) Engels, B.; Peyerimhoff, S. D. *J. Phys. Chem.* **1989**, *93*, 4462.
(23) Pasto, D. J.; Krasnansky, R.; Zercher, C. *J. Org. Chem.* **1987**, *52*, 3062.
(24) Bernardi, F.; Bottoni, A.; Fossey, J.; Sorba, J. *J. Mol. Struct.* **1985**, *119*, 231.
(25) Schlegel, H. B. *J. Phys. Chem.* **1982**, *86*, 4678.
(26) Fossey, J.; Nedelec, J.-Y. *Tetrahedron* **1981**, *37*, 2967.
(27) Kato, S.; Morokuma, K. *J. Chem. Phys.* **1980**, *72*, 206.
(28) Pross, A.; Radom, L. *Tetrahedron* **1980**, *36*, 1999.
(29) Radom, L.; Paviot, J.; Pople, J. A. *J. Chem. Soc. Chem. Commun.* **1974**, 58.
(30) Hoffmann, R.; Radom, L.; Pople, J. A.; Schleyer, P. v. R.; Hehre, W. J.; Salem, L. *J. Am. Chem. Soc.* **1972**, *94*, 6221.
(31) Guerra, M. *J. Am. Chem. Soc.* **1992**, *114*, 2077.
(32) Bernardi, F.; Fossey, J. *J. Mol. Struct.* **1988**, *180*, 79.
(33) Guerra, M. *Chem. Phys. Lett.* **1987**, *139*, 463.
(34) Clark, T.; Symons, M. C. R. *J. Chem. Soc. Chem. Commun.* **1986**, 96.
(35) Engels, B.; Peyerimhoff, S. D. *J. Mol. Struct.* **1986**, *138*, 59.
(36) Molino, L. M.; Poblet, J. M.; Canadell, E. *J. Chem. Soc., Perkin Trans. 2* **1982**, 1217.
(37) Chen, Y.; Tschuikow-Roux, E. *J. Phys. Chem.* **1992**, *96*, 7266.
(38) Engels, B.; Peyerimhoff, S. D.; Skell, P. S. *J. Phys. Chem.* **1990**, *94*, 1267.
(39) Bernardi, F.; Bottoni, A.; Fossey, J.; Sorba, J. *Tetrahedron* **1986**, *42*, 5567.
(40) Hoz, T.; Sprecher, M.; Basch, H. *J. Phys. Chem.* **1985**, *89*, 1664.
(41) Schlegel, H. B.; Sosa, C. *J. Phys. Chem.* **1984**, *88*, 1141.
(42) Hopkinson, A. C.; Lien, M. H.; Csizmadia, I. G. *Chem. Phys. Lett.* **1980**, *71*, 557.
(43) Biddles, I.; Hudson, A. *Chem. Phys. Lett.* **1973**, *18*, 45.
(44) Creary, X. *Advances in Carbocation Chemistry*; JAI Press: London, 1989; Vol. I.
(45) Raghavachari, T.; Haddon, R. C.; Jr, W. H. S. *J. Am. Chem. Soc.* **1982**, *104*, 5054.
(46) Reynolds, C. H. *J. Am. Chem. Soc.* **1992**, *114*, 8676.
(47) Skell, P. S.; Traynham, J. G. *Acc. Chem. Res.* **1984**, *17*, 160.
(48) Skell, P. S.; Shea, K. J. *Bridged Free Radicals*; Kochi, J. K., Ed.; John Wiley & Sons: New York, 1973.
(49) Krusic, P. J.; Kochi, J. K. *J. Am. Chem. Soc.* **1971**, *93*, 846.
(50) Lloyd, R. V.; Wood, D. E. *J. Am. Chem. Soc.* **1975**, *97*, 5986.
(51) Lysons, A. R.; Symons, M. C. R. *J. Am. Chem. Soc.* **1971**, *93*, 7330.
(52) von Onciul, A.; Clark, T. *J. Chem. Soc. Chem. Commun.* **1989**, 1082.
(53) Chen, Y.; Rauk, A.; Tschuikow-Roux, E. *J. Chem. Phys.* **1990**, *93*, 1187.
(54) Jaguar 3.0; Schrödinger, Inc.: Portland, OR, 1997. Greeley, B. H.; Russo, T. V.; Mainz, D. T.; Friesner, R. A.; Langlois, J.-M.; Goddard, W. A., III; Donnelly, R. E.; Ringnalda, M. N. *J. Chem. Phys.* **1994**, *101*, 4028. Tannor, D. J.; Marten, B.; Murphy, R.; Friesner, R. A.; Sitkoff, D.; Nicholls, A.; Ringnalda, M.; Goddard, W. A., III; Honig, B. *J. Am. Chem. Soc.* **1994**, *116*, 11875.
(55) Hay, P. J.; Wadt, W. R. *J. Chem. Phys.* **1985**, *82*, 284.

(56) Møller, C.; Plesset, M. S. *Phys. Rev.* **1934**, *46*, 618.
(57) Sæbø, S.; Pulay, P. *Annu. Rev. Phys. Chem.* **1993**, *44*, 213.
(58) Murphy, R. B.; Beachy, M. D.; Friesner, R. A.; Ringnalda, M. N. *J. Chem. Phys.* **1995**, *103*, 1481.
(59) Becke, A. D. *Phys. Rev. A* **1988**, *38*, 3098.
(60) Slater, J. C. *Quantum Theory of Molecules and Solids*; McGrow-Hill: New York, 1974.
(61) Vosko, S. H.; Wilk, L.; Nusair, M. *Can. J. Phys.* **1980**, *58*, 1200.
(62) Lee, C.; Yang, W.; Parr, R. G. *Phys. Rev. B* **1988**, *37*, 785.
(63) Perdew, J. P.; Chevary, J. A.; Vosko, S. H.; Jackson, K. A.; Pederson, M. R.; Singh, D. J.; Fiolhais, C. *Phys. Rev. B* **1992**, *46*, 6671.
(64) Modelli, A.; Scagnolari, F.; Distefano, G.; Guerra, M.; Jones, D. *Chem. Phys.* **1990**, *145*, 89.
(65) Nathanson, G. M.; Minton, T. K.; Shane, S. F.; Lee, Y. T. *J. Chem. Phys.* **1989**, *90*, 6157.
(66) Cao, J.; Ihee, H.; Zewail, A. H. *Proc. Natl. Acad. Sci.* **1999**, *96*, 338.
(67) Ihee, H.; Kua, J.; Zewail, A. H.; Goddard, W. A., III In preparation.
(68) Castelhano, A. L.; Marriott, P. R.; Griller, D. *J. Am. Chem. Soc.* **1981**, *103*, 4262.
(69) *JANAF Thermochemical Tables, Natl. Stand. Ref. Data. Ser. U.S. Natl. Bur. Stand. 37*; 2nd ed.; U. S. GPO: Washington D.C., 1971.
(70) Schlegel, H. B.; Bhalla, K. C.; Hase, W. L. *J. Phys. Chem.* **1982**, *86*, 4883.
(71) Holmes, J. L.; Lossing, F. P. *J. Am. Chem. Soc.* **1988**, *110*, 7343.
(72) Franklin, J. A.; Huybrechts, G. H. *Int. J. Chem. Kinet.* **1969**, *1*, 3.
(73) Ihee, H.; Zewail, A. H. Work in progress.